Current Research in Food Science 8 (2024) 100671

Contents lists available at ScienceDirect

Current Research in Food Science

journal homepage: www.sciencedirect.com/journal/current-research-in-food-science

Effects of high-pressure processing on the physicochemical and adsorption properties, structural characteristics, and dietary fiber content of kelp (*Laminaria japonica*)

Songlin Zhao [a], Zhitao Pan [b], Nima Azarakhsh [a], Hosahalli S. Ramaswamy [c], Hanying Duan [b,*], Chao Wang [b,**]

[a] International School, Jinan University, Guangzhou, 510632, China
[b] Department of Food Science and Technology, Jinan University, Guangzhou, 510632, China
[c] Department of Food Science and Agricultural Chemistry, Macdonald Campus of McGill University, Montréal, QC, Canada

ARTICLE INFO

Keywords:
Kelp
High-pressure processing
Physicochemical properties
Soluble dietary fiber
Particle size
Microstructure

ABSTRACT

To investigate the effects of high-pressure processing (HPP) on the physicochemical and adsorption properties and structural characteristics of kelp, kelp slice (KS) and kelp powder (KP) were treated under different pressures (300, 450, and 600 MPa) for 5 and 10 min. Compared to untreated KP, HPP-treated KP yielded a 1.31-fold increase in water holding capacity (600 MPa/5 min), a 0.12-fold increase in swelling capacity (450 MPa/10 min), a 1.33-fold increase in oil holding capacity (600 MPa/10 min), a 10-fold increase in glucose adsorption capacity (450 MPa/10 min), and a 0.22-fold increase in cholesterol adsorption capacity (163.1 mg/g DW at 450 MPa/10 min), and exhibited good Cd (II) adsorption capacity when its concentration was 10 mmol/L in the small intestine. The physicochemical properties of HPP-treated KS were not improved due to its low specific surface area. In addition, HPP treatment efficiently reduced the particle size of KP and increased its total and soluble dietary fiber content by 17% and 63% at 600 MPa/10 min, respectively. Scanning electron microscope micrographs demonstrated that the surface of HPP-treated KP was rough and porous, and the specific surface area increased with increasing pressure and processing time. To conclude, the results obtained in the present study suggest that HPP is a promising processing method for improving the functionality and structural characteristics of KP and provide a theoretical basis for the utilization of HPP-treated KP as a fiber-rich ingredient in the functional food industry.

1. Introduction

Kelp (*Laminaria japonica*), also known as kombu and Yangtze cabbage, is mainly produced in coastal areas of the Liaodong Peninsula and Shandong Peninsula, and the production of kelp in China ranks first in the world (Li et al., 2022a). However, significant amounts of kelp resources are wasted due to underutilization. The wasted kelp often ends up on the beach and exerts many negative impacts, such as producing rotten odors, contributing to red tide, and becoming an environmental pollutant (Sunwoo et al., 2017). Kelp has a high nutritional value and is a premium source of several polysaccharides, vitamins, minerals, and other nutrients, exhibiting many positive physiological benefits, including anti-inflammation, anti-obesity, and anti-diabetes (Shirosaki and Koyama, 2011). Dietary fiber (DF), comprising soluble dietary fiber (SDF) and insoluble dietary fiber (IDF), is a nondigestible polysaccharide derived from plants that exhibits strong hydration and adsorption properties and serves a crucial function in the gastrointestinal tract, including maintaining well-balanced gut microbial ecology, increasing fecal volume, adsorbing and quickly excreting excess glucose, lipids, and toxic substances, and reducing the occurrence of cardiovascular disease, stroke, and diabetes (Gill et al., 2021; Makki et al., 2018). Recent studies have demonstrated that either SDF or IDF derived from *L. japonica* could alleviate chronic diseases such as diabetes and obesity in mice by increasing the abundance of beneficial bacteria (e.g., *Akkermansia*) and decreasing the abundance of pernicious bacteria (e.g., *Staphylococcus*) through fermentation, which produced short-chain fatty

* Corresponding author.
** Corresponding author.
E-mail addresses: tduhy@jnu.edu.cn (H. Duan), chao_wang@jnu.edu.cn (C. Wang).

https://doi.org/10.1016/j.crfs.2023.100671
Received 29 October 2023; Received in revised form 13 December 2023; Accepted 26 December 2023
Available online 27 December 2023

acids and lowered the pH (Wang et al., 2022; Zhang et al., 2021). Although both SDF and IDF have many health benefits, SDF has shown more positive effects in increasing viscosity, forming gels, and providing better texture and taste and is generally considered more important than IDF (Chen and Wu, 2022). However, IDF accounts for a large proportion of most plant-based foods, so the conversion of IDF to SDF by appropriate processing methods is imperative for the advancement of functional food products.

More recently, a range of processing methods have been employed to enhance the functionality of DF in food products, encompassing but not limited to high-pressure processing (HPP), high-pressure homogenization, twin-screw extrusion, and ball milling (Chen and Wu, 2022; Wang et al., 2020; Xiao et al., 2021). HPP is an emerging nonthermal processing technology that physically treats materials at a pressure of 100–1000 MPa using a pressure-transmitting medium (Spotti and Campanella, 2017). The application of HPP in food industries initially focused on microbial destruction leading to nonthermal pasteurization and sterilization (Zhao et al., 2022). HPP can alter the noncovalent bonds (hydrogen, ionic, and hydrophobic bonds) of biomacromolecules in foods, thereby inducing changes in their structural characteristics; moreover, it has almost no influence on monosaccharides formed by high-energy covalent bonds (Huang et al., 2020). A previous study demonstrated that both IDF and SDF content of HPP-treated apple byproducts increased significantly, with the SDF:IDF ratio increasing from 52.9% to 65.7% (De la Peña Armada et al., 2020). Sheng et al. (2017) found that the particle size of HPP-treated grape pomace was comparatively smaller than that of untreated grape pomace and exhibited a more lamellar structure with a large number of holes on the surface. Yan et al. (2019) reported that subjecting pear pomace to HPP treatment at 300 MPa for 15 min resulted in a 67.8% increase in water holding capacity, a 52.2% increase in oil holding capacity, and a 55.0% increase in swelling capacity compared to untreated pear pomace. In general, HPP has been considered an efficient method to enhance the quality of DF, and the role of HPP in the modification of food products has now been gradually emphasized. However, to the best of our knowledge, the impact of HPP on raw kelp and its DF has not been reported.

The objective of the present study was to treat kelp with HPP and subsequently evaluate the effects of different HPP conditions on the physicochemical properties (water holding capacity, oil holding capacity, and swelling capacity), adsorption properties (glucose adsorption capacity, cholesterol adsorption capacity, and toxic ion adsorption capacity), and structural characteristics of kelp. In addition, the total dietary fiber (TDF) content and the individual contents of SDF and IDF were determined. It is our hope that these findings not only provide a theoretical basis for the modification of kelp with HPP for further industrial application but also offer a new perspective on the comprehensive exploitation and utilization of kelp resources to reduce pollution of the marine environment.

2. Materials and methods

2.1. Materials

Fresh kelp (*Laminaria japonica*), fresh eggs (Charoen Pokphand Food, Charoen Pokphand Group), and corn oil (Fulinmen, China Oil and Foodstuffs Corporation) were obtained from a local supermarket in Guangzhou, Guangdong, China. Alkaline protease, glucose, and cholesterol standards were obtained from Aladdin Biochemical Technology Co., Ltd. (Shanghai, China). α-amylase, glucoamylase, and Rochelle salt were obtained from Sigma-Aldrich Trading Co., Ltd. (Shanghai, China). Cadmium (II) chloride, copper (II) sulfate, hydrochloric acid, sulfuric acid, glacial acetic acid, sodium hydroxide, and absolute ethanol were of analytical grade and purchased from Damao Chemical Reagent Factory (Tianjin, China).

2.2. HPP treatment of raw kelp

The treatment of raw kelp was performed according to the flow chart in the Supplementary Material (Fig. S1). The fresh raw kelp was washed twice with distilled water, cut into rectangular pieces (3 cm × 8 cm), put into food-grade PET/PE (polyethylene terephthalate/polyethylene) bags, and vacuum packaged. Subsequently, the sealed samples were subjected to an ultrahigh-pressure machine (CQC−2 L−600 full liquid phase ultrahigh pressure food sterilizer, Beijing Suyuan Zhongtian Scientific, Ltd., Beijing, China) and treated at 300, 450, and 600 MPa for 5 and 10 min, respectively. The pressure vessel was maintained at ambient temperature (25 °C). The HPP system was fully programmable, allowing reproducible pressure buildup and decompression times. The pressure ramp-up time was 120 s, and the decompression time was 60 s. Since the temperature of foods with high moisture content generally increases by approximately 3 °C per 100 MPa of compression during HPP, samples were precooled to 18, 12, and 4 °C for 300, 450, and 600 MPa treatments, respectively, to achieve similar final processing temperatures (30 °C) at different pressures (Wu et al., 2023). The pressure buildup and decompression times were not included in the processing time. Each HPP condition was conducted in triplicate. The control groups were prepared without HPP. All HPP-treated and untreated samples were freeze-dried for 48 h using a freeze dryer (SCIENTZ−18N, Ningbo Scientz Biotechnology Co., Ltd., Ningbo, China) to obtain kelp slice (KS) samples. Then, a portion of the freeze-dried KS samples from each condition was ground to obtain kelp powder (KP) samples. All samples were stored at 4 °C for further analysis.

2.3. Physicochemical properties

2.3.1. Water holding capacity (WHC) and oil holding capacity (OHC)

The WHC and OHC were determined according to the method described by Speroni et al. (2020) with some modifications. A total of 0.2 g of sample was mixed with 10 mL of distilled water or 5 g of corn oil in a centrifugal tube, stirred at room temperature for 1 h, and centrifuged at 10000 rpm for 10 min in a high-speed centrifuge (ST 16R high-speed refrigerated centrifuge, Guangzhou Yuanqi Biotechnology Co., Ltd., Guangzhou, China). WHC and OHC were then calculated according to Equations (1) and (2).

$$WHC(g/g\ DW) = \frac{m_1 - m_0}{m_0} \tag{1}$$

where m_1 is the sample weight after water holding (g) and m_0 is the dry weight (DW) of the sample (g).

$$OHC(g/g\ DW) = \frac{m_1 - m_0}{m_0} \tag{2}$$

where m_1 is the sample weight after oil holding (g) and m_0 is the dry weight of the sample (g).

2.3.2. Swelling capacity (SC)

The SC was determined according to the method described by Li et al. (2022b) with some modifications. A total of 0.2 g of sample was weighed into a 15 mL graduated cylinder and mixed with 10 mL of distilled water. After stirring, the mixture was incubated at room temperature for 24 h. SC was then calculated according to Equation (3).

$$SC(mL/g\ DW) = \frac{V_1 - V_0}{m_0} \tag{3}$$

where V_0 and V_1 are the volume of the sample before and after swelling (mL), respectively, and m_0 is the dry weight of the sample (g).

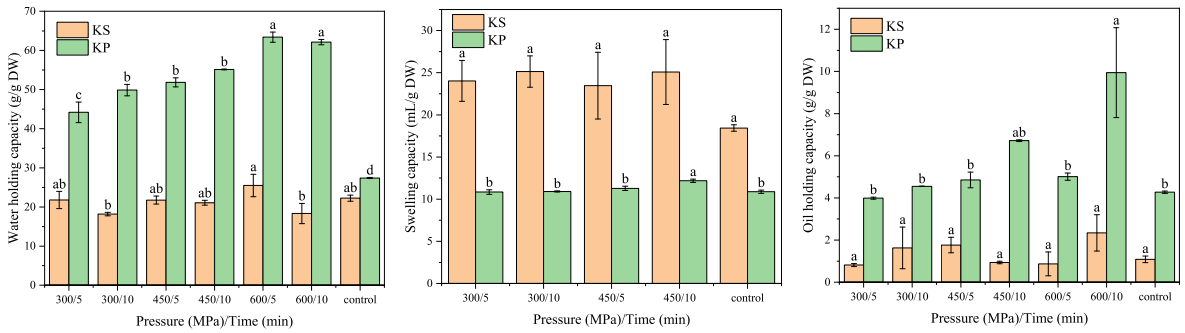

Fig. 1. Water holding capacity (a), swelling capacity (b), and oil holding capacity (c) of untreated and HPP-treated kelp slice (KS) and kelp powder (KP). Either untreated or HPP-treated samples were gone through freeze-drying and grinding as shown in Fig. S1. Data were expressed as the mean ± standard deviation (SD) of nine measurements and were expressed on a dry weight (DW) basis. Values with different letters in the bars of the same color indicated significant differences ($P < 0.05$). (For interpretation of the references to color in this figure legend, the reader is referred to the Web version of this article.)

2.4. Adsorption properties

2.4.1. Glucose adsorption capacity (GAC)

The GAC was determined according to the method described by Qiao et al. (2021) with some modifications. A total of 0.2 g of sample was fully mixed with 20 mL of 0.5 mol/L glucose solution, incubated in a thermostatic water bath machine (HH−2, Jintan Honghua Instrument Factory, Jintan, China) at 37 °C for 6 h, and centrifuged at 10,000 rpm for 10 min. The supernatant was recovered, and the glucose content in the supernatant was determined by the 3,5-dinitrosalicylic acid (DNS) colorimetric method. Briefly, 0.5 mL of the recovered supernatant was transferred into a centrifuge tube, followed by mixing with 2.5 mL of distilled water and 2 mL of DNS reagent (prepared by mixing 5 g of DNS, 8 g of sodium hydroxide, and 150 g of Rochelle salt in 500 mL of distilled water). The mixture was then incubated at 100 °C for 5 min with constant shaking. After the mixture was cooled to room temperature, the glucose content was measured at 520 nm using a UV–Vis spectrophotometer (UV-1900, Shimadzu, Kyoto, Japan). GAC was calculated according to Equation (4).

$$GAC(g/g\ DW) = \frac{m_1 - m_2}{m_0} \tag{4}$$

where m_1 and m_2 are the glucose content in the solution before and after adsorption (g), respectively, and m_0 is the dry weight of the sample (g).

2.4.2. Cholesterol adsorption capacity (CAC)

The CAC was determined according to the method described by Gan et al. (2021) with some modifications. A total of 0.3 g of sample was mixed with 15 mL of diluted yolk solution (a fresh egg yolk whipped and homogenized with 4-fold volumes of distilled water) in a centrifuge tube, and the pH was adjusted to 7.0. Then, the mixture was incubated at 37 °C for 120 min and centrifuged at 4000×*g* for 4 min. The absorbance of the supernatant was measured at 550 nm and quantified based on the calibration curve ($y = 0.1757x + 0.1373$, $R^2 = 0.9909$). CAC was then calculated according to Equation (5).

$$CAC(mg/g\ DW) = \frac{m_1 - m_2}{m_0} \tag{5}$$

where m_1 and m_2 are the cholesterol content of the egg yolk emulsion before and after adsorption (mg), respectively, and m_0 is the dry weight of the sample (g).

2.4.3. Toxic ion adsorption capacity (TIAC)

The TIAC of Cd (II) and Cu (II) was determined according to the method described by Wang et al. (2015) with some modifications. When determining the maximum binding capacity (BC_{max}), 0.05 g of sample was mixed with 10 mL of a solution containing 10 mmol/L of $CdCl_2$ and $CuSO_4$. Then, the pH of the solution was adjusted to 2.0 and 7.0 to simulate the *in vivo* environment of the stomach and intestine, respectively. Subsequently, the mixture was incubated in a water bath at 37 °C for 3 h with constant shaking (120 rpm). The supernatant was collected after centrifuging at 4000×*g* for 10 min, and 2 mL was then mixed with 8 mL of absolute ethanol to precipitate SDF. Finally, the concentrations of Cd (II) and Cu (II) in the resultant supernatant were determined by an inductively coupled plasma-mass spectrometer (7700x model, Agilent Technologies, Santa Clara, CA, USA). When determining the minimum binding capacity (BC_{min}), 0.125 g of sample and 500 μmol/L of $CdCl_2$ and $CuSO_4$ were used, and all other conditions were the same as for BC_{max}. TIAC was then calculated according to Equation (6).

$$TIAC(mg/g\ DW) = \frac{(C_1 - C_0) \times V}{m_0} \tag{6}$$

where C_0 and C_1 are the initial and equilibrium concentrations of the metal ion (mg/L), respectively; V is the volume of added solution (L); and m_0 is the dry weight of the sample (g).

2.5. TDF, IDF, and SDF contents

The TDF, IDF, and SDF contents were determined following the AOAC official method 991.43 (AOAC, 1994).

2.6. Structural characteristics

2.6.1. Particle size distribution

The particle size distribution of KP was determined by a laser diffraction particle size analyzer (SALD−2300, Shimadzu, Kyoto, Japan). KP (0.1 g) was dispersed in 10 mL of distilled water, and the suspension was sonicated for 5 min before being subjected to a particle size analyzer.

2.6.2. Scanning electron microscopy (SEM)

The microstructure of KP was observed using a scanning electron microscope (XL−30 ESEM FEG, FEI Company, Hillsboro, OR, USA). Prior to observation, KP was attached to double-sided conducting adhesive tape and coated with gold-palladium alloy. The scanning images were captured at an accelerating voltage of 5.00 kV and photographed at 3000× magnification under low vacuum.

2.6.3. X-ray diffraction (XRD)

The XRD analysis of KP was carried out according to the method

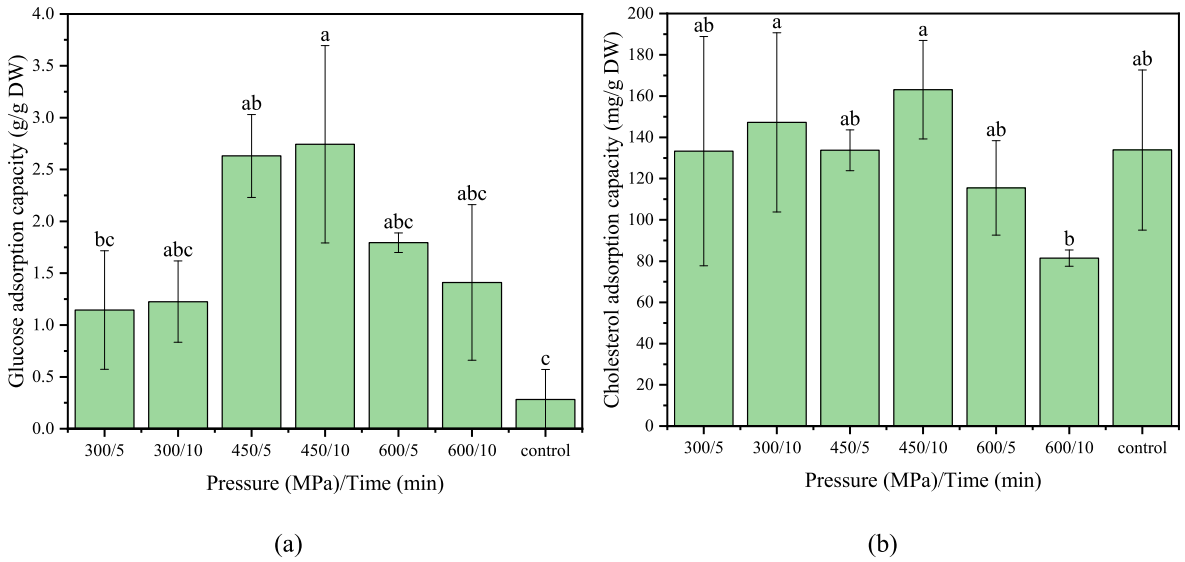

Fig. 2. Glucose adsorption capacity (a) and cholesterol adsorption capacity (b) of kelp powder of untreated and HPP-treated kelp powder. Either untreated or HPP-treated samples were gone through freeze-drying and grinding as shown in Fig. S1. Data were expressed as the mean ± standard deviation (SD) of nine measurements and were expressed on a dry weight (DW) basis. Values with different letters indicated significant differences ($P < 0.05$).

described by Ge et al. (2022) with some modifications. The XRD patterns were obtained by an X-ray diffractometer (D8 advance, Bruker, Karlsruhe, Germany) with a Cu-Kα radiation source (λ = 1.542 Å) running at a working voltage and current of 40 kV and 40 mA, respectively. The scanning rate was 2°/min, and the diffraction angle (2θ) range was 0–80°. The crystallinity index was calculated by MDI Jade 6.0 (Materials Data, Inc., Livermore, CA, USA).

2.7. Statistical analysis

Tests for samples from each HPP condition were conducted in nine replicates (three replicates of HPP treatments for each condition and three replicates of samples for each HPP treatment). Data are expressed as the mean ± standard deviation (SD), and one-way analysis of variance (ANOVA) followed by *post hoc* Tukey's honestly significant difference (HSD) test was conducted to determine the statistical significance of means among different treatment groups at $P < 0.05$ using Minitab 20.0 (Minitab, Inc., State College, PA, USA).

3. Results and discussion

3.1. Effect of HPP treatment on physicochemical properties

High WHC and SC can increase fecal volume, promote bowel movements, alleviate intestinal pressure, and are effective in the prevention of intestinal diseases (Xiao et al., 2021). The WHC and SC of untreated KS, HPP-treated KS, untreated KP, and HPP-treated KS are shown in Fig. 1a and b. In comparison to untreated KS, the WHC of HPP-treated KS did not exhibit any significant difference. In contrast, the WHC of HPP-treated KP increased significantly ($P < 0.05$), with the highest value being 63.4 g/g DW (600 MPa/5 min), which was 1.31-fold higher than that of untreated KP (27.4 g/g DW). The WHC of other materials treated with HPP, such as pomelo fruitlets DF and pickled vegetables IDF, were 1.11 times and 1.18 times that of untreated ones, respectively, which was in agreement with our study (Li et al., 2020; Ouyang et al., 2023). Interestingly, the SC values of the KS groups were higher than those of the KP groups, which might be due to the presence of free water in the crevices of KS, thus resulting in larger measured values than the actual values. The SC of HPP-treated KP significantly increased ($P < 0.05$) to 12.2 mL/g (450 MPa/10 min), which was 12% higher than that of untreated KP (10.9 mL/g). Except for the condition of 450 MPa/10 min, the SC of the other HPP-treated KP groups did not show a significant difference. Compared to asparagus pomace (3.42 mL/g) treated by superfine grinding (Gao et al., 2020), either untreated or HPP-treated KP (10.8−12.2 mL/g) showed much higher SC but lower than HPP-treated purple-fleshed potato (16.1 mL/g) (Xie et al., 2017), which might be due to the differences in the physical structure, SDF content, or processing methods of the materials. HPP is effective in breaking hydrogen bonds in the IDF of KP, converting it to SDF, which can absorb more water and form a gel-like substance. With increasing pressure and processing time, the specific surface area of KP increased, and polar groups and other water-binding sites were exposed, resulting in improved WHC and SC (Chau et al., 2007; Fayaz et al., 2022).

The OHC is related to the stabilization of high-fat products and emulsions and the capacity to reduce serum cholesterol levels (Elleuch et al., 2011; Yan et al., 2019). OHC of KS and KP before and after modification is shown in Fig. 1c. Similar to WHC and SC, no significant difference was observed between treated and untreated KS ($P > 0.05$). The maximum OHC value of HPP-treated KP reached 9.94 g/g DW (600 MPa/10 min), which was 1.33-fold higher than that of untreated KP (4.27 g/g DW). Compared with HPP-treated KP, lower OHC was found in olive pomace treated by ball milling (1.2 g/g) and wheat bran treated by twin-screw extrusion (2.75 g/g) (Speroni et al., 2020; Wang et al., 2020). In addition, the results showed that the OHC of KP treated by HPP for 5 min did not show a significant difference at all pressures, whereas significant differences were observed after 10 min of treatment at 450 MPa and 600 MPa ($P < 0.05$). A previous study reported that the OHC of deoiled cumin DF treated by HPP for 25 min increased with increasing pressure, which could be attributed to the increased processing time, resulting in an increase in porosity and the exposure of significant amounts of buried hydrophobic groups inside the cumin DF (Ma and Mu, 2016). Therefore, increasing the processing time may be an effective way to improve the OHC of KP.

The differences in the specific surface area of KS and KP have an impact on their physicochemical properties. The dispersion and specific surface area of KP increased after grinding, making KP more susceptible to being influenced by HPP treatment. In contrast, KS had a denser structure, making it difficult to expose hydrophilic or hydrophobic groups by HPP treatment, so the physicochemical properties of KS groups were mostly inferior to those of KP groups (except SC). Therefore, in the subsequent results and discussions, only KP was chosen as the raw material for the present study.

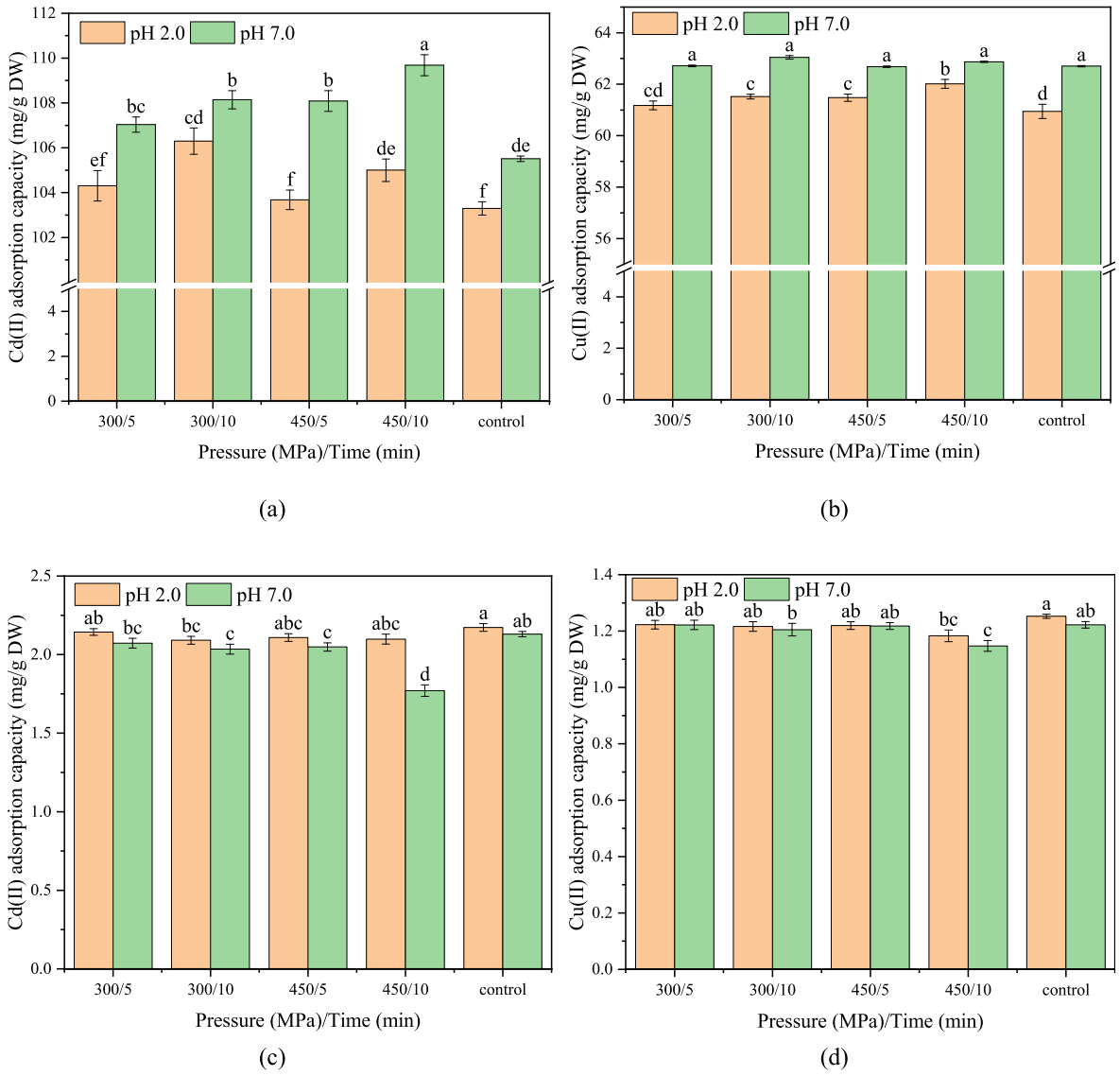

Fig. 3. The maximum binding capacity of Cd (II) (a) and Cu (II) (b), and the minimum binding capacity of Cd (II) (c) and Cu (II) (d) of untreated and HPP-treated kelp powder. Either untreated or HPP-treated samples were gone through freeze-drying and grinding as shown in Fig. S1. Data were expressed as the mean ± standard deviation (SD) of nine measurements and were expressed on a dry weight (DW) basis. Values with different letters in the bars of the same color indicated significant differences ($P < 0.05$). (For interpretation of the references to color in this figure legend, the reader is referred to the Web version of this article.)

3.2. Effect of HPP treatment on adsorption properties

3.2.1. GAC

The ability of food to bind glucose can reduce the digestion and absorption of glucose in the intestine, thus inhibiting the occurrence of postprandial hyperglycemia (Li et al., 2022b; Yu et al., 2018). The results in Fig. 2a show that the GAC of all HPP-treated KP increased, exhibiting a tendency to increase and then decrease with increasing pressure, although significant differences were observed only in the groups treated at 450 MPa for 5 min and 10 min ($P < 0.05$). The highest value of GAC for HPP-treated KP was 2.74 g/g DW (450 MPa/10 min), which was 10-fold higher than that of untreated KP (0.24 g/g DW). HPP treatment could increase the exposure of hydrophilic groups such as hydroxyl, carboxyl, and uronic acid groups in side chains, which provided more sites for binding glucose via van der Waals forces and hydrogen bonds (Ouyang et al., 2023). Unlike WHC, a decrease in GAC was observed as the pressure increased to 600 MPa, which was probably due to the alteration of the spatial network structure of KP (Li et al., 2020). Although the improvements of both WHC and GAC are associated with the exposure of hydrophilic groups, HPP treatment may disrupt the specific binding sites for glucose by inducing conformational changes on the surface of KP, whereas water holding capacity was unaffected by these binding sites. In addition, the pore size of KP might decrease, making it suitable for water molecules but not large enough to accommodate glucose molecules. These results were in agreement with a previous study reported by Yu et al. (2018) on carrot pomace IDF.

3.2.2. CAC

Excess cholesterol and deposition can lead to obesity, cardiovascular disease, and liver cirrhosis (Qiao et al., 2021). The CAC of KP before and after modification is shown in Fig. 2b. Although the maximum CAC value of HPP-treated KP (163.1 mg/g DW, 450 MPa/10 min) was higher than that of untreated KP (133.9 mg/g DW), it did not cause a significant difference ($P > 0.05$). It is worth noting that the factors contributing to the higher OHC and CAC are not the same. The OHC is mainly affected by the structural characteristics of the food material, such as porosity and specific surface area, whereas CAC can be influenced by not only the structural characteristics but also by the interactions between

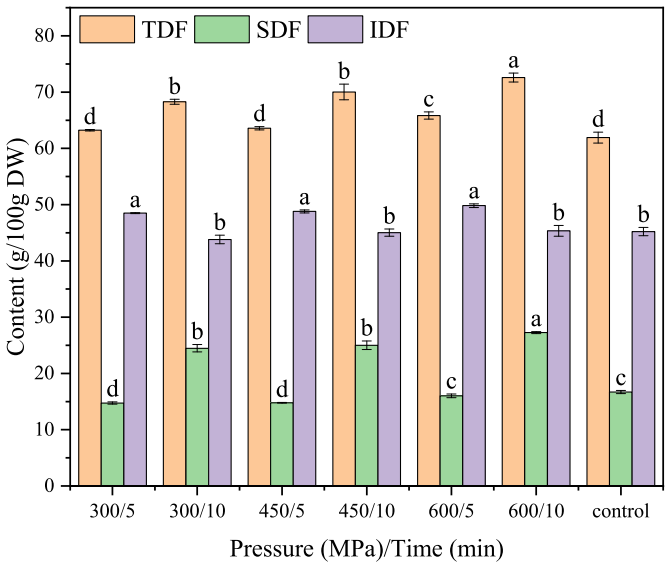

Fig. 4. Total dietary fiber (TDF), soluble dietary fiber (SDF), and insoluble dietary fiber (IDF) content of untreated and HPP-treated kelp powder. Either untreated or HPP-treated samples were gone through freeze-drying and grinding as shown in Fig. S1. Data were expressed as the mean ± standard deviation (SD) of nine measurements and were expressed on a dry weight (DW) basis. Values with different letters in the bars of the same color indicated significant differences ($P < 0.05$). (For interpretation of the references to color in this figure legend, the reader is referred to the Web version of this article.)

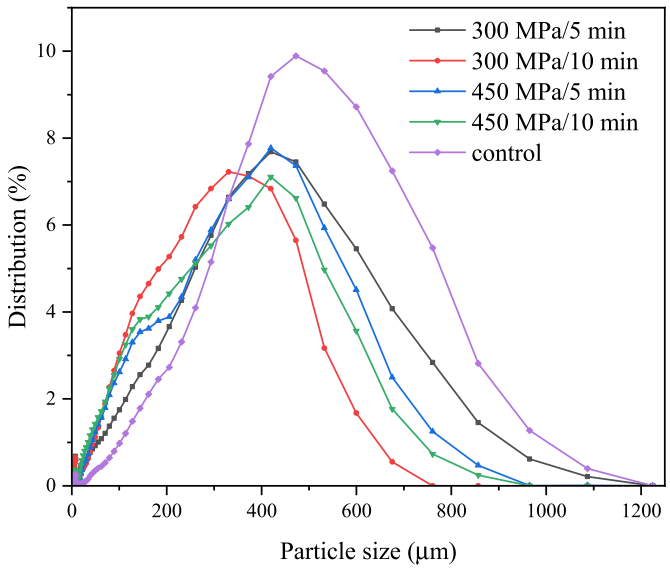

Fig. 5. Particle size distribution of untreated and HPP-treated kelp powder. Either untreated or HPP-treated samples were gone through freeze-drying and grinding as shown in Fig. S1.

cholesterol and certain components, such as SDF content, in the food material (Benitez et al., 2019; Yu et al., 2023); this explains why the OHC of HPP-treated KP is 1.33-fold higher than that of untreated KP, while there was no significant difference observed in CAC. Similarly, KP treated at 300 MPa for 10 min also exhibited higher CAC, and these improvements could be related to the higher SDF content in KP (Fig. 4). SDF can dissolve in water and form a viscous gel, which traps or binds cholesterol and thus improves the CAC of the food material (Benitez et al., 2019; Trautwein and McKay, 2020). However, when the pressure reached 600 MPa, KP aggregated, thus restricting the binding of DF to cholesterol.

3.2.3. TIAC

BC_{max} is the level at which all the binding sites of the DF are saturated by the toxic ions; BC_{min} is the equilibrium concentration at which the amount of ions bound by the DF is equal to the amount of ions released by the DF, provided that the binding sites of the DF are not saturated with toxic ions (Zhang et al., 2011). As shown in Fig. 3a and b, the BC_{max} values of KP for two toxic ions at pH 7.0 were significantly higher than those at pH 2.0 ($P < 0.05$), indicating that KP had a higher affinity for toxic ions in the intestine than in the stomach. Moreover, at pH 7, compared to untreated KP (105.5 mg/g DW), the adsorption capacity of HPP-treated KP for Cd (II) increased to 109.7 mg/g DW (450 MPa/10 min). The small intestine is a more important location in determining the detoxification capacity of DF since food and toxic substances remain in the small intestine much longer than in the stomach (Ou et al., 1999). As the pH increased, the carboxyl or hydroxyl groups dissociated to carboxyl or hydroxyl anions, which formed stronger interactions with toxic ions and thus increased the adsorption capacity (Ge et al., 2022). However, there was no significant difference in the adsorption capacity for Cu (II) at pH 7 ($P > 0.05$); this could be attributed to the unique coordination chemistry of the surface of KP, which had a relatively low affinity for Cu (II), although HPP treatment could induce more polar groups exposed to the surface. Additionally, although BC_{min} decreased when the pH increased from 2.0 to 7.0, it still remained high, indicating that KP was not able to adsorb Cd (II) and Cu (II) effectively when their concentrations were relatively low in the intestine. Nevertheless, it is worth noting that HPP treatment could significantly lower the adsorption capacity of the BC_{min} of KP for both Cd (II) and Cu (II) at pH 7 at 450 MPa/10 min compared to untreated KP.

3.3. Effect of HPP treatment on TDF, SDF, and IDF content

The TDF, SDF, and IDF contents of untreated and HPP-treated KP are shown in Fig. 4. The maximum TDF content reached 72.6 g/100 g DW (600 MPa/10 min), which was 17% higher than that of untreated KP (61.9 g/100 g DW) and much higher than that of wheat bran (45.95 g/100 g) treated by twin-screw extrusion (Wang et al., 2020). The IDF content of KP treated with HPP for 5 min at all pressures increased significantly ($P < 0.05$), whereas the SDF content did not show any significant difference or even decreased. SDF is evenly distributed across the cell and comprises mainly oligosaccharides and pectin, whereas IDF is primarily located in the cell wall and comprises mainly cellulose, hemicellulose, and lignin (Chen and Wu, 2022). A previous study demonstrated that some small-molecular-weight oligosaccharides may be lost during HPP treatment, leading to a decrease in SDF content (Sang et al., 2022). In addition, HPP treatment could physically disrupt the cell wall of KP, thereby releasing the entrapped IDF. As the processing time increased to 10 min, the IDF content decreased significantly, and the SDF content increased significantly ($P < 0.05$), suggesting that HPP treatment could induce cellulose degradation and convert IDF to SDF (Xie et al., 2017). These results were consistent with a previous study reported by Sheng et al. (2017) on grape pomace.

3.4. Effect of HPP treatment on structural characteristics

3.4.1. Particle size distribution

As shown in Fig. 5, the particle size of all KP groups was approximately normally distributed, with the peak located at 300–500 μm. Compared to untreated KP (395.13 μm), a smaller median particle size was observed in all HPP-treated KP groups, with the smallest being only 209.94 μm (300 MPa/10 min). Although the modes of particle size of the other three KP groups (300 MPa/5 min, 450 MPa/5 min, and 450 MPa/10 min) were all 419.58 μm, the number of particles below 419.58 mm was obviously increased with increasing pressure and processing time (Fig. 5). These results indicated that HPP treatment could effectively reduce the particle size of KP by damaging the microstructure and

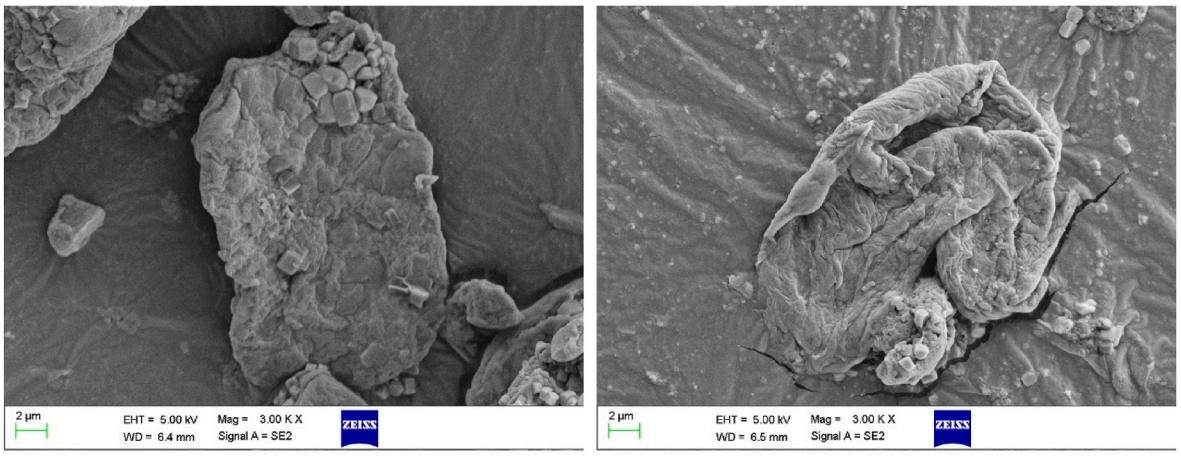

a) 300 MPa/5 min b) 300 MPa/10 min

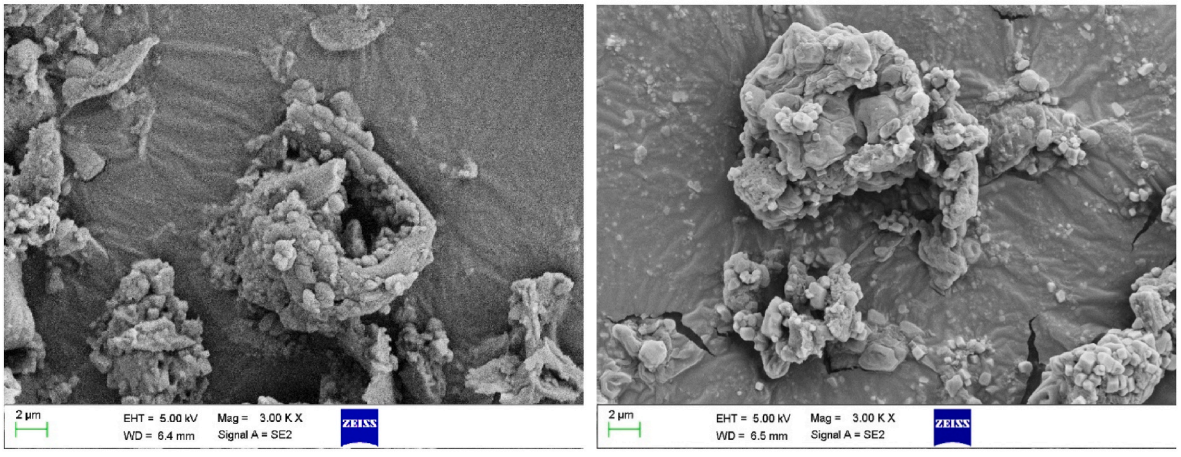

c) 450 MPa/5 min d) 450 MPa/10 min

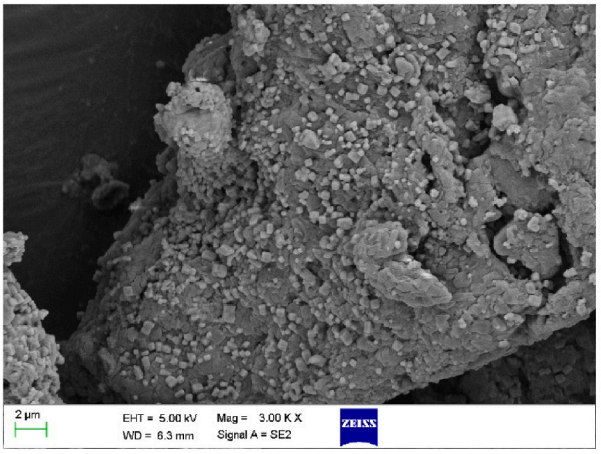

e) control

Fig. 6. Scanning electron micrographs (3000 ×) of untreated and HPP-treated kelp powder. Either untreated or HPP-treated samples were gone through freeze-drying and grinding as shown in Fig. S1.

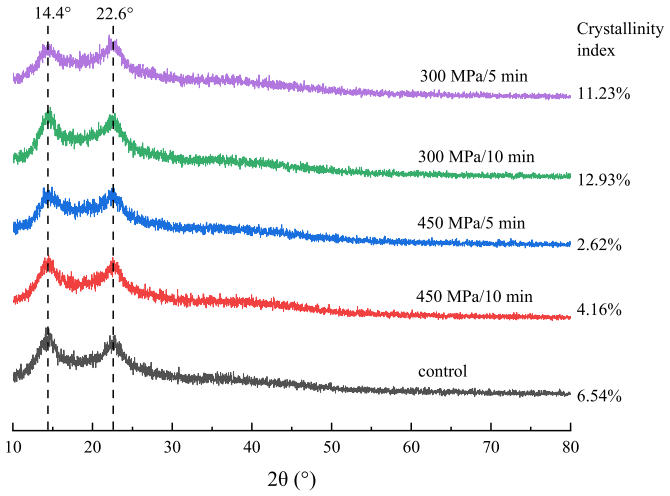

Fig. 7. X-ray diffraction patterns of untreated and HPP-treated kelp powder. Either untreated or HPP-treated samples were gone through freeze-drying and grinding as shown in Fig. S1. 2θ represents the diffraction angle.

cleaving the noncovalent bonds in the macromolecules to form smaller fragments (Sang et al., 2022). It is worth noting that freeze-drying and grinding also had an impact on the particle size of KP, as the sublimation of frozen water created a porous internal structure, leading to finer powders obtained after grinding (Ando and Nei, 2023).

3.4.2. SEM

SEM micrographs of untreated and HPP-treated KP are shown in Fig. 6. The untreated KP exhibited a relatively smooth and regular surface with a compact structure. In contrast, the surface of HPP-treated KP was rough and porous, and crushing and fracture structures could be observed. In addition, as the pressure and processing time increased, the inner structure of KP was gradually exposed, and the specific surface area increased. The loose and porous structure of HPP-treated KP allowed more hydrophilic and hydrophobic groups to be fully exposed, thus improving its ability to bind water, oil, glucose, and other substances (Sheng et al., 2017). This finding is in good accordance with the results of the physicochemical and adsorption properties, which showed that the WHC, SC, OHC, and GAC of KP were improved by HPP treatment. Meanwhile, as mentioned earlier, freeze-drying also contributed to the formation of the porous structure of KP (Ando and Nei, 2023).

3.4.3. XRD

The XRD patterns and crystallinity indices of untreated and HPP-treated KP are shown in Fig. 7. All KP groups exhibited strong peaks at 2θ diffraction angles of approximately 22.6° and 14.4°, which were attributed to the typical crystal structure of cellulose I. Although no difference was observed in the peak positions of HPP-treated KP, the variation in peak heights indicated that different HPP conditions could produce different results, i.e., disruption of crystalline or amorphous regions.

The crystallinity index of KP treated at 300 MPa for 10 min was 98% higher than that of untreated KP, suggesting that HPP treatment could induce the removal of lignin and hemicellulose from the crystal structure of cellulose I, thus forming a more regular crystal structure and increasing the crystallinity (Ouyang et al., 2023). As the pressure increased, the crystallinity index of KP decreased rapidly to only 40% (450 MPa/5 min) of untreated KP, indicating that HPP treatment was able to break the intermolecular hydrogen bonds between neighboring cellulose molecules and expose the internal amorphous regions of KP at 450 MPa (Xiao et al., 2021).

4. Conclusions

HPP is an effective processing method to improve the physicochemical and adsorption properties as well as the structural characteristics of KP. As the pressure and processing time increased, the particle size of KP decreased, and the structure became looser, which allowed more water and oil binding sites to be exposed, resulting in higher WHC, SC, and OHC values, which were 1.31-fold (600 MPa/5 min), 0.12-fold (450 MPa/10 min), and 1.33-fold (600 MPa/10 min) higher than those of untreated KP. The XRD analyses also suggested that the internal amorphous regions of KP were exposed at 450 MPa. On the other hand, KS had a compact structure with a low specific surface area, so the effect of HPP treatment on its physicochemical properties was not significant. The GAC of HPP-treated KP was 10-fold (450 MPa/10 min) higher than that of untreated KP, showing good potential in preventing the occurrence of postprandial hyperglycemia, while CAC did not show significant improvement. Additionally, KP exhibited good adsorption capacity for Cd (II) when its concentration in the small intestine was 10 mmol/L. The TDF content of HPP-treated KP increased significantly, and the conversion of IDF to SDF was observed at all pressures when the processing time increased to 10 min. The above results suggested that HPP could promote the functionality of KP, with the most prominent and comprehensive effect at 450 MPa/10 min. Overall, HPP-treated KP can be used as a fiber-rich ingredient in baked goods or beverages due to its capacity to bind water, fat, and glucose. Future studies could explore the possible *in vivo* effects of HPP-treated KP, such as hyperglycemia and promotion of intestinal health, to broaden their applications in functional food products.

CRediT authorship contribution statement

Songlin Zhao: Methodology, Investigation, Formal analysis, Writing – original draft. **Zhitao Pan:** Validation. **Nima Azarakhsh:** Formal analysis, Writing – review & editing. **Hosahalli S. Ramaswamy:** Conceptualization, Writing – review & editing, Formal analysis. **Hanying Duan:** Supervision, Conceptualization, Writing – review & editing. **Chao Wang:** Supervision, Conceptualization, Writing – review & editing, Funding acquisition.

Declaration of competing interest

The authors declare that they have no known competing financial interests or personal relationships that could have appeared to influence the work reported in this paper.

Data availability

No data was used for the research described in the article.

Acknowledgements

This research is supported by Key-Area Research and Development Program of Chaozhou City (No. 202202ZD03), Key-Area Research and Development of Heyuan City (No. 2022010) and Innovative Projects for university teachers (2021JNHB12).

Appendix A. Supplementary data

Supplementary data to this article can be found online at https://doi.org/10.1016/j.crfs.2023.100671.

References

Ando, Y., Nei, D., 2023. Comparison of potato void structures dried by air-drying, freeze-drying, and microwave-vacuum-drying, and the physical properties of powders after grinding. Food Bioprocess Technol. 16, 447–458. https://doi.org/10.1007/s11947-022-02941-x.

AOAC, 1994. AOAC Official Method 991.43. Total, Soluble, and Insoluble Dietary Fiber in Foods. Association of Official Analytical Chemists, Washington DC.

Benitez, V., Rebollo-Hernanz, M., Hernanz, S., Chantres, S., Aguilera, Y., Martin-Cabrejas, M.A., 2019. Coffee parchment as a new dietary fiber ingredient: functional and physiological characterization. Food Res. Int. 122, 105–113. https://doi.org/10.1016/j.foodres.2019.04.002.

Chau, C.-F., Wang, Y.-T., Wen, Y.-L., 2007. Different micronization methods significantly improve the functionality of carrot insoluble fibre. Food Chem. 100, 1402–1408. https://doi.org/10.1016/j.foodchem.2005.11.034.

Chen, Y.R., Wu, S.J., 2022. Effects of high-hydrostatic pressure and high-pressure homogenization on the biological activity of cabbage dietary fiber. J. Sci. Food Agric. 102, 6299–6308. https://doi.org/10.1002/jsfa.11980.

De la Peña Armada, R., Villanueva-Suárez, M.J., Mateos-Aparicio, I., 2020. High hydrostatic pressure processing enhances pectin solubilisation on apple by-product improving techno-functional properties. Eur. Food Res. Technol. 246, 1691–1702. https://doi.org/10.1007/s00217-020-03524-w.

Elleuch, M., Bedigian, D., Roiseux, O., Besbes, S., Blecker, C., Attia, H., 2011. Dietary fibre and fibre-rich by-products of food processing: characterisation, technological functionality and commercial applications: a review. Food Chem. 124, 411–421. https://doi.org/10.1016/j.foodchem.2010.06.077.

Fayaz, G., Soleimanian, Y., Mhamadi, M., Turgeon, S.L., Khalloufi, S., 2022. The applications of conventional and innovative mechanical technologies to tailor structural and functional features of dietary fibers from plant wastes: a review. Compr. Rev. Food Sci. Food Saf. 21, 2149–2199. https://doi.org/10.1111/1541-4337.12934.

Gan, J., Xie, L., Peng, G., Xie, J., Chen, Y., Yu, Q., 2021. Systematic review on modification methods of dietary fiber. Food Hydrocolloids 119, 106872. https://doi.org/10.1016/j.foodhyd.2021.106872.

Gao, W., Chen, F., Zhang, L., Meng, Q., 2020. Effects of superfine grinding on asparagus pomace. Part I: changes on physicochemical and functional properties. J. Food Sci. 85, 1827–1833. https://doi.org/10.1111/1750-3841.15168.

Ge, Q., Li, H., Huang, L., Li, P., Xiao, Z., Jin, K., 2022. Structure, physicochemical, and *in vitro* functional properties of insoluble dietary fiber from bamboo culm: a potential functional ingredient. J. Food Process. Preserv. 46, e16426 https://doi.org/10.1111/jfpp.16426.

Gill, S.K., Rossi, M., Bajka, B., Whelan, K., 2021. Dietary fibre in gastrointestinal health and disease. Nat. Rev. Gastroenterol. Hepatol. 18, 101–116. https://doi.org/10.1038/s41575-020-00375-4.

Huang, H.W., Hsu, C.P., Wang, C.Y., 2020. Healthy expectations of high hydrostatic pressure treatment in food processing industry. J. Food Drug Anal. 28, 1–13. https://doi.org/10.1016/j.jfda.2019.10.002.

Li, H., Yi, Y., Guo, S., Zhang, F., Yan, H., Zhan, Z., Zhu, Y., Duan, J., 2022a. Isolation, structural characterization and bioactivities of polysaccharides from *Laminaria japonica*: a review. Food Chem. 370, 131010 https://doi.org/10.1016/j.foodchem.2021.131010.

Li, M., Liu, Y., Yang, G., Sun, L., Song, X., Chen, Q., Bao, Y., Luo, T., Wang, J., 2022b. Microstructure, physicochemical properties, and adsorption capacity of deoiled red raspberry pomace and its total dietary fiber. LWT–Food Sci. Technol. 153, 112478 https://doi.org/10.1016/j.lwt.2021.112478.

Li, W., Jin, Q., Wu, Q., Zhang, W., Luo, Y., Gu, S., Wu, J., Wang, Z., 2020. Effect of a hybrid process, high hydrostatic pressure treatment combined with mixed-strain fermentation, on the quality of the dietary fibre in pickled vegetables. Int. J. Food Sci. Technol. 55, 2650–2659. https://doi.org/10.1111/ijfs.14518.

Ma, M., Mu, T., 2016. Modification of deoiled cumin dietary fiber with laccase and cellulase under high hydrostatic pressure. Carbohydr. Polym. 136, 87–94. https://doi.org/10.1016/j.carbpol.2015.09.030.

Makki, K., Deehan, E.C., Walter, J., Backhed, F., 2018. The impact of dietary fiber on gut microbiota in host health and disease. Cell Host Microbe 23, 705–715. https://doi.org/10.1016/j.chom.2018.05.012.

Ou, S., Gao, K., Li, Y., 1999. An *in vitro* study of wheat bran binding capacity for Hg, Cd, and Pb. J. Agric. Food Chem. 47, 4714–4717. https://doi.org/10.1021/jf9811267.

Ouyang, H., Guo, B., Hu, Y., Li, L., Jiang, Z., Li, Q., Ni, H., Li, Z., Zheng, M., 2023. Effect of ultra-high pressure treatment on structural and functional properties of dietary fiber from pomelo fruitlets. Food Biosci. 52, 102436 https://doi.org/10.1016/j.fbio.2023.102436.

Qiao, H., Shao, H., Zheng, X., Liu, J., Liu, J., Huang, J., Zhang, C., Liu, Z., Wang, J., Guan, W., 2021. Modification of sweet potato (*Ipomoea batatas* Lam.) residues soluble dietary fiber following twin-screw extrusion. Food Chem. 335, 127522 https://doi.org/10.1016/j.foodchem.2020.127522.

Sang, J., Li, L., Wen, J., Liu, H., Wu, J., Yu, Y., Xu, Y., Gu, Q., Fu, M., Lin, X., 2022. Chemical composition, structural and functional properties of insoluble dietary fiber obtained from the Shatian pomelo peel sponge layer using different modification methods. LWT–Food Sci. Technol. 165, 113737 https://doi.org/10.1016/j.lwt.2022.113737.

Sheng, K., Qu, H., Liu, C., Yan, L., You, J., Shui, S., Zheng, L., 2017. A comparative assess of high hydrostatic pressure and superfine grinding on physicochemical and antioxidant properties of grape pomace. Int. J. Food Sci. Technol. 52, 2106–2114. https://doi.org/10.1111/ijfs.13489.

Shirosaki, M., Koyama, T., 2011. *Laminaria japonica* as a food for the prevention of obesity and diabetes. Adv. Food Nutr. Res. 199–212. https://doi.org/10.1016/B978-0-12-387669-0.00015-6.

Speroni, C.S., Bender, A.B.B., Stiebe, J., Ballus, C.A., Ávila, P.F., Goldbeck, R., Morisso, F. D.P., Silva, L.P.d., Emanuelli, T., 2020. Granulometric fractionation and micronization: a process for increasing soluble dietary fiber content and improving technological and functional properties of olive pomace. LWT–Food Sci. Technol. 130, 109526 https://doi.org/10.1016/j.lwt.2020.109526.

Spotti, M.J., Campanella, O.H., 2017. Functional modifications by physical treatments of dietary fibers used in food formulations. Curr. Opin. Food Sci. 15, 70–78. https://doi.org/10.1016/j.cofs.2017.10.003.

Sunwoo, I.Y., Kwon, J.E., Nguyen, T.H., Ra, C.H., Jeong, G.T., Kim, S.K., 2017. Bioethanol production using waste seaweed obtained from Gwangalli Beach, Busan, Korea by co-culture of yeasts with adaptive evolution. Appl. Biochem. Biotechnol. 183, 966–979. https://doi.org/10.1007/s12010-017-2476-6.

Trautwein, E.A., McKay, S., 2020. The role of specific components of a plant-based diet in management of dyslipidemia and the impact on cardiovascular risk. Nutrients 12, 2671. https://doi.org/10.3390/nu12092671.

Wang, L., Xu, H., Yuan, F., Fan, R., Gao, Y., 2015. Preparation and physicochemical properties of soluble dietary fiber from orange peel assisted by steam explosion and dilute acid soaking. Food Chem. 185, 90–98. https://doi.org/10.1016/j.foodchem.2015.03.112.

Wang, X., Zhang, L., Qin, L., Wang, Y., Chen, F., Qu, C., Miao, J., 2022. Physicochemical properties of the soluble dietary fiber from *Laminaria japonica* and its role in the regulation of type 2 diabetes mice. Nutrients 14, 329. https://doi.org/10.3390/nu14020329.

Wang, Z., Yan, L., Ning, T., Wang, X., Li, R., Zhang, H., 2020. Increasing soluble dietary fiber content and antioxidant activity of wheat bran through twin-screw extrusion pretreatment. Prep. Biochem. Biotechnol. 50, 954–960. https://doi.org/10.1080/10826068.2020.1777424.

Wu, X., Tan, M., Zhu, Y., Duan, H., Ramaswamy, H.S., Bai, W., Wang, C., 2023. The influence of high pressure processing and germination on anti-nutrients contents, *in vitro* amino acid release and mineral digestibility of soybeans. J. Food Compos. Anal. 115, 104953 https://doi.org/10.1016/j.jfca.2022.104953.

Xiao, Z., Yang, X., Zhao, W., Wang, Z., Ge, Q., 2021. Physicochemical properties of insoluble dietary fiber from pomelo (*Citrus grandis*) peel modified by ball milling. J. Food Process. Preserv. 46, e16242 https://doi.org/10.1111/jfpp.16242.

Xie, F., Li, M., Lan, X., Zhang, W., Gong, S., Wu, J., Wang, Z., 2017. Modification of dietary fibers from purple-fleshed potatoes (*Heimeiren*) with high hydrostatic pressure and high pressure homogenization processing: a comparative study. Innovat. Food Sci. Emerg. Technol. 42, 157–164. https://doi.org/10.1016/j.ifset.2017.05.012.

Yan, L., Li, T., Liu, C., Zheng, L., 2019. Effects of high hydrostatic pressure and superfine grinding treatment on physicochemical/functional properties of pear pomace and chemical composition of its soluble dietary fibre. LWT–Food Sci. Technol. 107, 171–177. https://doi.org/10.1016/j.lwt.2019.03.019.

Yu, C., Dong, Q., Chen, M., Zhao, R., Zha, L., Zhao, Y., Zhang, M., Zhang, B., Ma, A., 2023. The effect of mushroom dietary fiber on the gut microbiota and related health benefits: a review. J. Fungi 9, 1028. https://doi.org/10.3390/jof9101028.

Yu, G., Bei, J., Zhao, J., Li, Q., Cheng, C., 2018. Modification of carrot (*Daucus carota* Linn. var. Sativa Hoffm.) pomace insoluble dietary fiber with complex enzyme method, ultrafine comminution, and high hydrostatic pressure. Food Chem. 257, 333–340. https://doi.org/10.1016/j.foodchem.2018.03.037.

Zhang, N., Huang, C., Ou, S., 2011. *In vitro* binding capacities of three dietary fibers and their mixture for four toxic elements, cholesterol, and bile acid. J. Hazard Mater. 186, 236–239. https://doi.org/10.1016/j.jhazmat.2010.10.120.

Zhang, Y., Zhao, N., Yang, L., Hong, Z., Cai, B., Le, Q., Yang, T., Shi, L., He, J., Cui, C., 2021. Insoluble dietary fiber derived from brown seaweed *Laminaria japonica* ameliorate obesity-related features *via* modulating gut microbiota dysbiosis in high-fat diet-fed mice. Food Funct. 12, 587–601. https://doi.org/10.1039/d0fo02380a.

Zhao, J., Zhang, Y., Chen, Y., Zheng, Y., Peng, C., Lin, H., Che, Z., Ding, W., 2022. Sensory and volatile compounds characteristics of the sauce in bean paste fish Treated with ultra-high-pressure and representative thermal sterilization. Foods 12, 109. https://doi.org/10.3390/foods12010109.